BOHR International Journal of Current research in Dentistry
2024, Vol. 3, No. 1, pp. 16–24
DOI: 10.54646/bijcrid.2024.23
www.bohrpub.com

ORIGINAL

Comparative evaluation of the accuracy of implant position reproduction obtained using analog and digital impression methods—an *in vitro* study

A. Sneha[1], Vidhya Jeyapalan[1]*, S. Jayakrishnakumar[1], Hariharan Ramakrishnan[2†], Vallabh Mahadevan[1] and Shivakumar Baskaran[3]

[1]Department of Prosthodontics and Implantology, Ragas Dental College and Hospital, Chennai, India
[2]Thai Moogambigai Dental College and Hospital, Dr. MGR Educational and Research Institute, Chennai, India
[3]Department of Periodontics, Ragas Dental College and Hospital, Chennai, India

***Correspondence:**
Vidhya Jeyapalan,
vidhya.mageshram@gmail.com

[†]**ORCID:**
Hariharan Ramakrishnan,
0000-0003-4466-5744

Received: 04 April 2024; **Accepted:** 12 July 2024; **Published:** 11 November 2024

Purpose of the study: To compare the accuracy of implant location reproduction utilizing digital and analog impression techniques.

Materials and methods: Two implant analogs were positioned bilaterally in the 2^{nd} premolar area at the crestal and 3 mm below the crestal level (subcrestal) to create a Maxillary Dentulous Master model. From the master model, ten analog implant impressions were created, and working castings with crestal (GROUP IA) and subcrestal (GROUP IB) implant analogs were produced. Using an intraoral scanner and STL files created, ten digital implant impressions were created from the master model with crestal (GROUP IIA) and subcrestal (GROUP IIB) implant analogs. The master model, or control, and the 10 working castings were digitalized and exported as STL files. By superimposing the STL files from each and every group onto the master model STL file, accuracy was evaluated. Using a gradient that was color-coded, the 3D deviations have been calculated at 10 different sites. The Mann–Whitney U test has been utilized statistically to assess the study's outcomes.

Results: There were no discernible variations in 3D deviations among GROUPS IA and IB, GROUPS IIA and IIB, and GROUPS IB and IIB. Only the distal contact area of the crestally implanted implant in the digital impressions showed statistically significant variations among GROUPS IA and IIA (P = 0.026), and this difference was judged to be within a threshold level that is clinically acceptable.

Conclusion: Both digital and analog implant impression techniques can be used for single-tooth implant impression making.

Keywords: bone implant interface, analogue digital conversion, dental impression technique, dental implant

Introduction

Dental implants have been routinely used to restore both fully and partially edentulous patients, expanding the range of fixed prosthetic treatment alternatives (1, 2) diagnosis and treatment planning, accuracy of impression, implant surgical procedures, passively fitting prosthesis, and maintenance can lead to predictable success in the field of implantology. The best geometric design, the most advantageous implant placement in relation to crestal bone, and the most efficient and reliable implant-abutment connection have all been the subject of numerous studies conducted in the field of implantology (2).

As per multiple authors, the preservation of the peri-implant crestal bone is a crucial element that ascertains the

stability of the surrounding soft tissue, ultimately resulting in improved esthetics and long-term efficacy (2). In order to avoid the exposure of the implant thread during bone remodeling and to give a sufficient esthetic emergence profile, some authors advocate placing the implant subcrestally. This has been shown to have a good impact on papilla formation and preservation of crestal bone (2, 3).

For implant-supported dental prostheses to be successful over the long term, a passive fit of the prosthesis is required (4). The initial stage toward accomplishing a passive fit for the implant prosthesis is taking a precise intraoral impression that mirrors the implant's three-dimensional orientation (5, 6). The implant angulation, number of implants, implant placement depth, utilization of closed or open impression trays, and material selection all affect how accurate the implant impression is (7).

To guarantee a precise fit for the prosthesis, impression copings from the implant have historically been transferred to the impression using "closed tray and open tray impression techniques (8, 9). The closed tray impression approach is used, when the implants are parallel to each other, and when there is a reduced interarch space. This method saves time, is easier for the operator, and much more comfortable for the patient in comparison to the open tray approach (7, 9). In the open tray impression approach, the copings will remain within the impression" once the set impression has been retrieved, which is one of the benefits of this method (10, 11). For a precise implant impression, vinyl polysiloxane and polyether were frequently utilized as impression materials. Silicone addition results in a more accurate impression than polyether, particularly for implants positioned deeply (8, 9, 12).

When combined with the stone cast, these analog high-precision impression materials—Polyether or Vinyl Polysiloxane—offer a tried-and-true technique for bringing the clinical setting into the lab (13). The traditional approach to creating impressions is widely used, straightforward, and equipment-light, but it is technique-sensitive. Inaccurate transfer of implant position can occur during laboratory procedures due to drawbacks like analogs' unstable repositioning, partial and extensive separation of impression material from the tray, impression distortion and shrinkage, and expansion of dental stone (9, 14).

The growth of CAD-CAM ("Computer-Aided Design and Computer-Aided Manufacturing") technology was aimed at providing a competitive edge over analog methods (13). The benefits of digital impressions include the removal of tray selection along with impression distortion, improved patient acceptance and comfort, and electronic storage due to the increased efficiency that comes with digital information (4, 14). Using an intraoral scanner (IOS) to convert intraoral situations into a virtual model, digital impressions are the initial stage of the digital workflow (15). The STL (Standard Tessellation Language) file, that is needed to produce the prosthesis, is created by the intraoral scanner (16).

Several authors have released studies (17–22) in which linear distance measurements have been utilized to examine the dental model's trueness. This method is not perfect though, as it cannot measure consistent reference points. CMMs (Coordinate Measuring Machines) were used by DeLong et al. to measure surface points with high trueness in order to assess the dental model's accuracy. However, their evaluation was limited because CMMs cannot scan in interproximal areas or fissure lines (23). In order to address the shortcomings of the earlier techniques used to gauge accuracy, STL datasets were obtained from the scanner, and software superimposition was used to compare the results.

Previous studies have compared the stone casts accuracy made from analog impressions and printed casts from digital impressions. Comparing the digital implant impression accuracy made with a variety of intraoral scanners to that of analog implant impression in partially edentulous individuals has only been done in a limited number of studies. Using the exposed scan body length as a basis for comparison, Na-Eun Nam et al. investigated the implant position reproduction accuracy at the time of optical scanning (15). Studies contrasting the accuracy of analog as well as digital impressions on implants positioned subcrestally and crestally, however, were limited.

Considering the aforementioned, the current study's objective was to compare the implant position reproduction accuracy attained through digital impression approaches versus analog approaches.

For implants positioned crestally and subcrestally, the null hypothesis states that there would be no appreciable variation in accuracy among analog and digital impressions.

Materials and methods

The dimensions of a 10*7*5 cm Maxillary Dentulous silicone mold (Ashoosons, Delhi, India) were chosen. To create the wax replica, modeling wax sheets were melted, poured into the dentulous silicone mold, and then allowed to cool. A wax knife was used to remove the left and right second premolars from the wax replica.

After that, the wax replica was set up and stabilized on the surveyor's (Saeshin Precision Ind. Co., Korea) surveying platform. In the wax replica, two implant analogs measuring 4 mm in diameter and 12 mm in length (NORIS DENTAL implants, Israel) have been placed at the right and left 2^{nd} premolar regions, parallel to each other and the insertion removal path. On the right second premolar region, the implant analog was positioned 3 mm subcrestally, while on the left second premolar region, it was positioned crestally.

The implant analogs and wax replica were placed inside a dental flask, dewaxed, filled with clear heat polymerizing acrylic resin (DPI, India), and cured in accordance with conventional guidelines.

FIGURE 1 | Intraoral scanner.

The polymerized acrylic model was taken out of the flask and polished and finished by utilizing acrylic trimmers "after the curing cycle was finished. Consequently, the completed acrylic model was acquired.

The two closed tray implant level impression copings (NORIS regular standard internal hex dental implants, Israel) have been screwed onto the acrylic model's implant analogs by utilizing a hex driver. To create closed tray implant level impressions, vinyl polysiloxane impression material in putty and light body consistencies (AVUE gum putty, light body, Korea)" was utilized. As instructed by the manufacturer, the impression was left alone for 3 min. The impression was removed from the acrylic model once the impression material had fully polymerized.

After removing the screws from the implant analogs of the acrylic model, the closed tray impression copings have been repositioned within the impression. Next, the closed tray impression copings have been attached to the implant analogs. Type IV dental stone was poured into the impression that held the left and right impression copings along with the implant analog assembly. The resulting cast served as the master model.

The master model subcrestal and crestal implant analogs have been linked to the closed tray implant level impression copings. Vinyl polysiloxane impression material has been utilized to create ten closed-tray implant-level impressions in total. The closed tray impression copings have been repositioned into the impression after being unscrewed from the master model implant analog. The impression copings were attached to the corresponding implant analogs. Type IV dental stone has been utilized to fill each of the ten impressions using the impression coping-implant analog assembly. Ten analog working casts in total were thus produced.

To attain a master model digital implant impression, the "scannable abutments (MIS, standard Internal hex Dentsply, India) which have been compatible with the chosen implant system have been linked to crestally and subcrestally placed implant analogs. The buccal wall was aligned with the flat surfaces of the scannable abutments. Using a higher-resolution 3D intraoral scanner (**Figure 1**, Medit i700 scanner, South Korea) at 10.9 μ ± 0.98 precision for 60 s without powder spraying, the master model containing the crestal along with subcrestal implant analogs was scanned". Before scanning, the scanner is calibrated in accordance with the manufacturer's instructions. To avoid mistakes, the manufacturer's recommended scanning path is adhered to. Beginning at the right side of the arch, the scanning path moves in a zigzag pattern toward the anterior region before scanning the contralateral scannable abutment at crestal implant analog in the direction of the terminal teeth. Next, the scannable abutment on the subcrestal implant analog is scanned at a 180° angle. The scannable abutments on both sides of the arch and the buccal as well as palatal surfaces of the teeth were scanned at 70–85° angulations after the contralateral terminal teeth were scanned. First, scannable abutments were not connected to the master model before scanning was performed again. Next, scannable abutments were connected to the crestal and subcrestal implant analogs. In this way, ten digital implant impressions were acquired. Next, an STL file is exported from the acquired image. Ten digital implant impressions were used to create ten STL files in a similar manner.

The resulting 20 test samples have been split into 2 groups of 10 samples each based on the impression-making technique. The implant analogs positioned crestally in each test sample were denoted as A, and the implant analogs positioned 3 mm subcrestally as B. The test samples were categorized as follows (**Figures 2**, **3**).

GROUP IA—working casts of implant analogs positioned crestally produced using the analog implant impression method.

GROUP IB—working casts of implant analogs positioned subcrestally produced using the analog implant impression method.

GROUP IIA—digital representations of implant analogs positioned crestally produced using a digital implant impression technique.

GROUP IIB—digital representations of implant analogs placed subcrestally, produced through the use of digital implant impression technology.

The ten analog working casts have been linked to the same scannable abutments at the crestal as well as subcrestal implant analogs using the same intraoral scanner that was previously used. Ten STL files were generated from the scanned images of the analog working casts, which were scanned using the same protocol as the digital implant impressions. The master model was digitally scanned once, and an STL file was created to act as a control when comparing the data. Using an automatic alignment mode, the STL datasets of every test sample from every group have

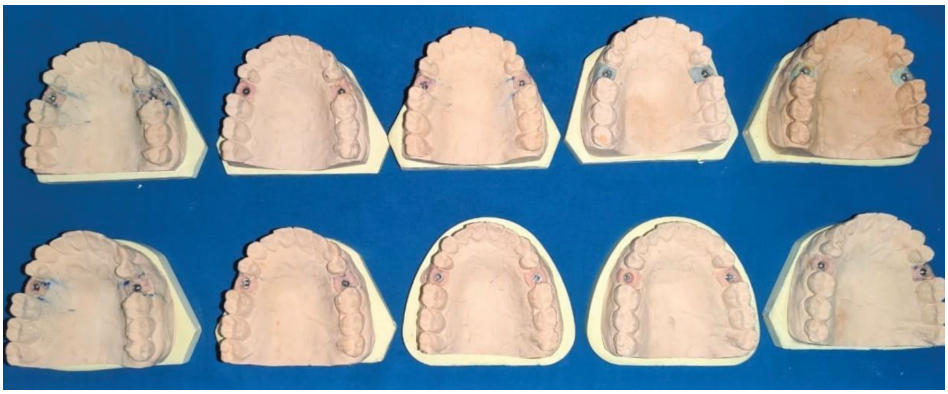

FIGURE 2 | GROUP IA–working casts of crestally placed implant generated from analog implant impression technique. GROUP IB–working casts of subcrestally placed implant generated from analog implant impression technique.

FIGURE 3 | GROUP IIA–Digital images of crestally placed implants generated from digital implant impression technique. GROUP IIB–Digital images of subcrestally placed implants generated from digital implant impression technique.

been individually aligned to the dataset of the master model. Software called Medit Compare Superimposition was then used to analyze the 3D deviations.

Each analog working cast's STL dataset was superimposed on top of the master model's STL dataset. At ten distinct locations, the 3D divergences among the master model and each analog working cast were calculated in the X, Y, and Z axes. The top of the scannable abutment, the mesial and distal interproximal contact points, the buccal and palatal cusps of the first premolar, the mesiobuccal and mesiopalatal cusps, the distal and mesial fossae of the first premolar, and the scannable abutment vertically are among the 10 particulars locations that were situated in the horizontal along with vertical axes adjacent to the site of implant. The precise locations were examined in 1 × 1 mm dimensions, and the 3D deviations were depicted using a gradient scale with color coding to show the difference in matching between the analog working casts and the master model (control). Each digital impression's STL dataset was superimposed on top of the master model's STL dataset. The X, Y, and Z axes have been calculated at the same ten precise locations as previously mentioned to determine the 3D deviations between each digital impression and the master model. The results are displayed on a gradient scale with colors.

Microsoft Excel 10 (Microsoft, USA) was used to tabulate the basic data and calculate the mean and standard deviation. The gathered data have been statistically evaluated by utilizing SPSS Software version 20.0 (SPSS Software Corp., Munich, Germany) for a test of significance. The Mann–Whitney U test has been utilized to evaluate accuracy within the group as well as between test groups.

Results

Tables 1–4 explain the basic data of all groups and their subgroups. **Tables 5, 6** were generated using Mann–Whitney tests. **Tables 7, 8** describe 3D deviations of crestally and subcrestally placed implants whose impressions were made using analog and digital methods. The 3D deviations of the specific locations in the working casts generated from analog implant impressions on crestally (GROUP IA, 11A) and subcrestally (GROUP IB, 11B) placed implants were found to be statistically insignificant. The 3D deviations of the digital impressions on the distal contact area of crestally placed implant were found to be higher than the working casts generated from analog impressions and this deviation was found to be significant, whereas the 3D deviations of the specific locations in working cast generated from analog (GROUP IB) implant impressions and digital implant impressions (GROUP IIB) on subcrestally placed implants were found to be statistically insignificant.

TABLE 1 | Mean values of the 3D deviations (mm) in the working casts generated from analog implant impressions on crestally placed implants (GROUP IA).

Samples	Buccal Cusp of 1^{st} premolar	Lingual cusp of 1st premolar	Mesio buccal cusp of 1^{st} molar	Mesio palatal cusp of 1^{st} molar	Top of scannable abutment	Scannable abutment vertical	Mesial fossae of 1^{st} molar	Distal fossae of 1st premolar	Mesial contact area of implant	Distal contact area of implant
1	0.003	0.001	0.003	0.002	0.001	0.002	−0.001	−0.002	− 0.003	− 0.001
2	0.003	0.004	0.001	0.001	0.002	0.001	−0.003	−0.003	−0.001	−0.001
3	0.002	0.003	0.002	0.002	0.001	0.002	−0.001	0.001	−0.002	−0.001
4	0.002	0.002	0.004	0.003	0.001	0.001	−0.002	−0.002	−0.002	−0.002
5	0.001	0.003	0.003	0.001	0.001	0002	−0.001	0.002	−0.003	−0.001
6	0.004	0.002	0.001	0.002	0.001	0.001	−0.002	−0.001	0.001	0.002
7	0.001	0.003	0.002	0.002	0.002	0.002	−0.003	−0.001	−0.001	−0.001
8	0.003	0.004	0.002	0.001	0.001	0.002	−0.001	−0.003	0.001	−0.002
9	0.004	0.004	0.002	0.002	0.001	0.003	−0.002	−0.001	−0.002	−0.001
10	0.002	0.001	0.002	0.001	0.003	0.002	0.001	−0.002	−0.003	− 0.002
Mean/SD	0.0025/ 0.001	0.0027/ 0.001	0.0022/ 0.002	0.0017/ 0.006	0.0014/ 0.004	0.0018/ 0.006	−0.0015 /0.001	−0.0012/ 0.001	−0.0015/ 0.002	−0.001/ 0.001

Inference: The Mean Values of the 3D deviations in Buccal Cusp of 1^{st} premolar, Lingual cusp of 1^{st} premolar, Mesiobuccal cusp of 1^{st} molar, Mesiopalatal cusp of 1^{st} molar, Top of scannable abutment, Scannable abutment vertical, Mesial fossae of 1^{st} molar, Distal fossae of 1^{st} premolar, Mesial contact area of implant and Distal contact area of implant were 0.0025, 0.0027, 0.0022, 0.0017, 0.0014, 0.0018, −0.0015, −0.0012, −0.0015 and −0.001mm, respectively.

TABLE 2 | Mean values of the 3D deviations (mm) in the Working casts generated from analog implant impressions on subcrestally placed implants (GROUP IB).

Samples	Buccal Cusp of 1st premolar	Lingual cusp of 1st premolar	Mesio buccal cusp of 1^{st} molar	Mesio palatal cusp of 1^{st} molar	Top of scannable abutment	Scannable abutment vertical	Mesial fossae of 1^{st} molar	Distal fossae of 1st premolar	Mesial contact area of implant	Distal contact area of implant
1	0.001	0.002	0.003	0.003	0.002	0.002	−0.003	− 0.002	− 0.003	−0.001
2	0.004	0.003	0.001	0.001	0.001	0.003	−0.001	−0.003	−0.001	−0.002
3	0.003	0.004	0.002	0.002	0.002	0.002	−0.002	0.001	−0.002	−0.001
4	0.002	0.004	0.003	0.003	0.001	0.003	− 0.002	−0.002	−0.001	−0.003
5	0.003	0.001	0.001	0.001	0.001	0.002	−0.003	0.002	−0.002	−0.003
6	0.002	0.002	0.001	0.002	0.002	0.001	0.001	−0.001	−0.001	−0.001
7	0.003	0.003	0.003	0.002	0.002	0.003	−0.002	−0.001	−0.002	−0.002
8	0.004	0.002	0.001	0.002	0.002	0.002	0.002	−0.003	−0.001	−0.001
9	0.004	0.003	0.002	0.002	0.001	0.003	−0.001	−0.001	−0.003	−0.003
10	0.001	0.001	0.003	0.003	0.002	0.003	0.001	−0.002	−0.003	−0.003
Mean/SD	0.0027/ 0.001	0.0025/ 0.001	0.002/ 0.001	0.0021/ 0.007	0.0016/ 0.0005	0.0024/ 0.0006	−0.001/ 0.0017	−0.0012/ 0.0016	−0.0019/ 0.0008	−0.002/ 0.001

Inference: The Mean Values of the 3D deviations in Buccal Cusp of 1^{st} premolar, Lingual cusp of 1^{st} premolar, Mesiobuccal cusp of 1^{st} molar, Mesiopalatal cusp of 1^{st} molar, Top of scannable abutment, Scannable abutment vertical, Mesial fossae of 1^{st} molar, Distal fossae of 1^{st} premolar, Mesial contact area of implant and Distal contact area of implant were 0.0027, 0.0025, 0.002, 0.0021, 0.0016, 0.0024, −0.001, −0.0012, −0.0019 and −0.002 mm, respectively.

Discussion

The implant prosthesis's passive fit, which is dependent on the implant impression accuracy, is essential to preventing mechanical issues (1). As a result, the durability of the finished restoration depends on a precise three-dimensional implant impression. The accurate fitting of the prosthesis is made simpler by the two commonly used impression techniques: the open tray as well as closed tray impression approaches. The traditional impression method is well-known, easy to use, and equipment-light, but it is technique-sensitive (9, 14).

The shortcomings of the traditional approach have a workable substitute in the form of the digital method. STL dataset serves as a foundation for CAD formation and is employed in the creation of precise implant prostheses (13).

TABLE 3 | Mean values of the 3D deviations (mm) in digital implant impressions on crestally placed implants (GROUP IIA).

Samples	Buccal Cusp of 1st premolar	Lingual cusp of 1st premolar	Mesio buccal cusp of 1st molar	Mesio palatal cusp of 1st molar	Top of scannable abutment	Scannable abutment vertical	Mesial fossae of 1st molar	Distal fossae of 1st premolar	Mesial contact area of implant	Distal contact area of implant
1	0.003	0.004	0.002	0.003	0.002	0.002	− 0.002	−0.001	− 0.003	− 0.003
2	0.001	0.001	0.003	0.001	0.001	0.002	−0.003	−0.003	−0.001	−0.001
3	0.002	0.003	0.001	0.002	0.001	0.003	0.001	−0.001	−0.002	−0.002
4	0.003	0.004	0.003	0.003	0.003	0.002	−0.002	−0.002	−0.001	−0.001
5	0.001	0.003	0.001	0.002	0.001	0.002	0.002	− 0.002	− 0.003	−0.002
6	0.004	0.002	0.002	0.003	0.002	0.002	−0.001	0.001	−0.001	−0.003
7	0.001	0.003	0.002	0.001	0.002	0.003	−0.001	−0.002	−0.002	−0.003
8	0.003	0.004	0.003	0.003	0.001	0.002	−0.003	0.002	−0.001	− 0.003
9	0.003	0.003	0.001	0.001	0.002	0.002	−0.001	−0.001	−0.002	−0.001
10	0.003	0.002	0.002	0.003	0.002	0.001	−0.001	−0.003	−0.002	−0.002
Mean/SD	0.0024/ 0.001	0.0029/ 0.009	0.002/ 0.008	0.0022/ 0.001	0.0017/ 0.006	0.0021/ 0.005	−0.0011/ 0.001	−0.0012/ 0.002	−0.0018/ 0.007	−0.0021/ 0.007

Inference: The Mean Values of the 3D deviations in Buccal Cusp of 1st premolar, Lingual cusp of 1st premolar, Mesiobuccal cusp of 1st molar, Mesiopalatal cusp of 1st molar, Top of scannable abutment, Scannable abutment vertical, Mesial fossae of 1st molar, Distal fossae of 1st premolar, Mesial contact area of implant and Distal contact area of implant were 0.0024, 0.0029, 0.002, 0.0022, 0.0017, 0.0021, −0.0011, −0.0012, −0.0018 and −0.0021 mm, respectively.

TABLE 4 | Mean values of the 3D deviations (mm) in digital implant impressions on subcrestally placed implants (GROUP IIB).

Samples	Buccal Cusp of 1st premolar	Lingual cusp of 1st premolar	Mesio buccal cusp of 1st molar	Mesio palatal cusp of 1st molar	Top of scannable abutment	Scannable abutment vertical	Mesial fossae of 1st molar	Distal fossae of 1st premolar	Mesial contact area of implant	Distal contact area of implant
1	0.001	0.003	0.004	0.003	0.001	0.002	−0.001	−0.003	−0.002	−0.001
2	0.004	0.002	0.003	0.001	0.003	0.001	−0.002	−0.001	−0.003	− 0.002
3	0.001	0.003	0.001	0.002	0.001	0002	0.001	−0.002	−0.002	−0.002
4	0.003	0.004	0.001	0.001	0.002	0.001	−0.001	− 0.002	−0.001	−0.001
5	0.004	0.004	0.002	0.003	0.002	0.002	−0.003	−0.003	−0.003	−0.003
6	0.001	0.003	0.002	0.003	0.003	0.002	−0.001	0.001	−0.003	−0.003
7	0.004	0.002	0.003	0.001	0.001	0.003	−0.002	−0.002	− 0.003	− 0.001
8	0.001	0.003	0.001	0.002	0.002	0.002	0.002	− 0.002	−0.001	−0.001
9	0.003	0.004	0.001	0.003	0.003	0.001	−0.001	0.001	−0.002	−0.001
10	0.001	0.002	0.003	0.001	0.001	0.002	−0.003	−0.001	− 0.003	−0.001
Mean/SD	0.002/ 0.001	0.003/ 0.001	0.002/0. 001	0.02/ 0.002	0.0019/ 0.001	0.0018/ 0.002	−0.0011/ 0.001	−0.0014/ 0.001	−0.0023/ 0.001	−0.0016/ 0.0008

Inference: The Mean Values of the 3D deviations in Buccal Cusp of 1st premolar, Lingual cusp of 1st premolar, Mesiobuccal cusp of 1st molar, Mesiopalatal cusp of 1st molar, Top of scannable abutment, Scannable abutment vertical, Mesial fossae of 1st molar, Distal fossae of 1st premolar, Mesial contact area of implant and Distal contact area of implant were 0.002, 0.003, 0.002, 0.02, 0.0019, 0.0018, −0.0011, −0.0014, −0.0023 and −0.0016 mm, respectively.

In the current study, vinyl polysiloxane impression material from the master model was used to create ten analog implant impressions using a closed tray impression technique. Delong et al. state that impression digitization has not been advised because of the impression's shape, the elastic qualities of the impression material, and the potential for error due to interaction with the digitization source (23). According to the manufacturer's instructions, ten scannable Type IV dental stones were used to create ten working casts from the ten impressions.

With a high precision of 10.9 μ ± 0.98, 10 digital impressions have been created from the master model by utilizing the Medit i700 intraoral scanner and scannable abutments. For the emergence profile scan, scannable abutments have been first scanned without being connected. After that, the abutments were scanned and STL files were produced. The master model and the analog working casts were digitized and then exported as STL files.

By superimposing each group's STL file onto the master model STL file using Medit Compare software's automatic

TABLE 5 | Comparative evaluation of 3D deviations (mm) in working casts generated from analog implant impressions on crestally (GROUP IA) and subcrestally (GROUP IB) placed implants using Mann–Whitney U test.

Locations	Crestal		Subcrestal		*P*-value
	Mean	SD	Mean	SD	
Buccal Cusp of 1^{st} premolar	0.0025	0.00108	0.0027	0.00116	0.667
Lingual cusp of 1^{st} premolar	0.0027	0.00116	0.0025	0.00108	0.667
Mesiobuccal cusp of 1^{st} molar	0.0022	0.000919	0.002	0.000943	0.691
Mesiopalatal cusp of 1^{st} molar	0.0017	0.000675	0.0021	0.000738	0.217
Top of scannable abutment	0.0014	0.000699	0.0016	0.000516	0.302
Scannable abutment Vertical	0.0018	0.000633	0.0024	0.000699	0.058
Mesial fossae of 1^{st} molar	−0.0015	0.001179	−0.001	0.001764	0.668
Distal fossae of 1^{st} premolar	−0.0012	0.001619	−0.0012	0.001619	1
Mesial contact area of implant	−0.0015	0.001509	−0.0019	0.000876	0.753
Distal contact area of implant	−0.001	0.001155	−0.002	0.000943	0.06

*P-value < 0.05 implies statistical significance.

TABLE 6 | Comparative evaluation of 3D deviations (mm) in digital implant impressions on crestally (GROUP IIA) and subcrestally (GROUP IIB) placed implants using Mann–Whitney *U* test.

Locations	Crestal		Subcrestal		*P*-value
	Mean	SD	Mean	SD	
Buccal Cusp of 1^{st} premolar	0.0024	0.001075	0.0023	0.001418	0.936
Lingual cusp of 1^{st} premolar	0.0029	0.000994	0.003	0.000817	0.905
Mesiobuccal cusp of 1^{st} molar	0.002	0.000817	0.0021	0.001101	0.905
Mesiopalatal cusp of 1^{st} molar	0.0022	0.000919	0.002	0.000943	0.625
Top of scannable abutment	0.0017	0.000675	0.0019	0.000876	0.626
Scannable abutment vertical	0.0021	0.000568	0.0018	0.000633	0.264
Mesial fossae of 1^{st} molar	−0.0011	0.001595	−0.0011	0.001595	1
Distal fossae of 1^{st} premolar	−0.0012	0.001619	−0.0014	0.00143	0.754
Mesial contact area of implant	−0.0018	0.000789	−0.0023	0.000823	0.173
Distal contact area of implant	−0.0021	0.000876	−0.0016	0.000843	0.194

*P-value < 0.05 implies statistical significance.

alignment mode, accuracy was evaluated. In order to achieve standardization and reproducibility, the 3-D deviations have been calculated in 10 specific locations that have been selected based on their clinical applications.

Papaspyridakos et al. state that the accuracy outcome may be impacted by the digital scanner, the digitization approach selected, and the alignment methods (22). In previous studies when comparing the digital and conventional approaches to the reference model, there were statistically significant variations in the fossae as well as vertical displacement of the implant. At ten designated contact locations, the milled models accuracy made from digital v/s gypsum casts made from traditional implant impressions was compared in this study (8, 24, 25). This discrepancy could be caused by differences in the operator's technique, the scanning path, the location of the implant within the dental arch, and the undercuts in the master cast. The distal contact area of implants placed crestally in the digital impressions in comparison to the analog impression approach showed statistically significant differences, according to the study's results (26).

When the implant was submerged at 3.00 mm, Na-Eun Nam et al. explained the accuracy of reproduction of implant spatial position in relation to variations in the scan body exposed length at crestal and different subcrestal levels and discovered that the precision was impacted (15). This contrasts with findings from the present investigation, which showed that accuracy at 3 mm subcrestal implant analog was unaffected.

The difference in true fit to a level of 150 μm is considered an acceptable threshold since it does not induce clinical complications. Many authors have adopted 100 μm as the threshold of a clinically accepted misfit (18–21). The current study found a statistically significant difference between the distal contact area of digital and analog

TABLE 7 | Comparative evaluation of 3D deviations (mm) in working casts generated from analog implant impressions (GROUP IA) and digital implant impressions (GROUP IIA) on crestally placed implants.

Locations	Analog		Digital		*P*-value
	Mean	SD	Mean	SD	
Buccal Cusp of 1^{st} Premolar	0.0025	0.00108	0.0024	0.001075	0.874
Lingual cusp of 1^{st} Premolar	0.0027	0.00116	0.0029	0.000994	0.723
Mesiobuccal cusp of 1^{st} molar	0.0022	0.000919	0.002	0.000817	0.687
Mesiopalatal cusp of 1^{st} molar	0.0017	0.000675	0.0022	0.000919	0.186
Top of scannable Abutment	0.0014	0.000699	0.0017	0.000675	0.251
Scannable abutment vertical	0.0018	0.000633	0.0021	0.000568	0.264
Mesial fossae of 1^{st} molar	−0.0015	0.001179	−0.0011	0.001595	0.607
Distal fossae of 1^{st} Premolar	−0.0012	0.001619	−0.0012	0.001619	1.000
Mesial contact area of implant	−0.0015	0.001509	−0.0018	0.000789	0.937
Distal contact area of implant	−0.001	0.001155	−0.0021	0.000876	**0.026***

**P*-value < 0.05 implies statistical significance.

TABLE 8 | Comparative evaluation of 3D deviations (mm) in working casts generated from analog implant impressions (GROUP IB) and digital implant impressions (GROUP IIB) on subcrestally placed implants.

Locations	Analog		Digital		*P*-value
	Mean	SD	Mean	SD	
Buccal Cusp of 1^{st} premolar	0.0027	0.00116	0.0023	0.001418	0.502
Lingual cusp of 1^{st} premolar	0.0025	0.00108	0.003	0.000817	0.286
Mesiobuccal cusp of 1^{st} molar	0.002	0.000943	0.0021	0.001101	0.872
Mesiopalatal cusp of 1^{st} molar	0.0021	0.000738	0.002	0.000943	0.81
Top of scannable abutment	0.0016	0.000516	0.0019	0.000876	0.459
Scannable abutment vertical	0.0024	0.000699	0.0018	0.000633	0.058
Mesial fossae of 1^{st} molar	−0.001	0.001764	−0.0011	0.001595	0.969
Distal fossae of 1^{st} premolar	−0.0012	0.001619	−0.0014	0.00143	0.754
Mesial contact area of implant	−0.0019	0.000876	−0.0023	0.000823	0.296
Distal contact area of implant	−0.002	0.000943	−0.0016	0.000843	0.323

P-value < 0.05 implies statistical significance.

impressions; however, the deviation (−2.1 μm) was within the threshold limit that is considered clinically acceptable. Thus, this study's null hypothesis is supported. There are not enough studies in the literature at the moment to allow for more comparisons between the accuracy of digital and conventional implant impressions on subcrestal implants.

There were not many restrictions on this study. The impact of blood, saliva, and gingival fluid—all of which are challenging to replicate *in vitro*—has not been examined in this study. Furthermore, the examination of different intraoral scanners, intraoral scan bodies, superimposition techniques, and implant systems was not included in this study. It was not determined how implant angulation affected accuracy. Additional research should be done using a larger sample size that includes more implants of different depths as well as alternative materials and impression techniques.

Conclusion

Comparable 3D accuracy was observed in working casts produced from digital and analog implant impressions. Based on the observations and results from this particular study, both methods of implant impression making are recommended. Digital implant impression making is a constantly evolving field and more future studies on similar kinds of topics will add more scientific value and evidence for the conclusion arrived for this current research.

Author contributions

AS and VJ: Collection of literature, concept and design, data collection, manuscript preparation, and editing. SJ: Sample preparation, collection of

articles, and manuscript preparation. HR: Manuscript editing, review. VM and SB: Manuscript review. All authors contributed to the article and approved the submitted version.

References

1. Osman M, Ziada H, Suliman A, Abubakr NH. A prospective clinical study on implant impression accuracy. *Int J Implant Dent.* (2019) 5:38.
2. Palacios-Garzón N, Velasco-Ortega E, López-López J. Bone loss in implants placed at subcrestal and crestal level: a systematic review and meta-analysis. *Materials.* (2019) 12:154.
3. de Siqueira R, Savaget Gonçalves R, Dos Santos P, de Mattias Sartori I, Wang H, Fontão F. Effect of different implant placement depths on crestal bone levels and soft tissue behavior: A 5-year randomized clinical trial. *Clin Oral Implants Res.* (2020) 31:282–93.
4. Alshawaf B, Weber H, Finkelman M, El Rafie K, Kudara Y, Papaspyridakos P. Accuracy of printed casts generated from digital implant impressions versus stone casts from conventional implant impressions: A comparative in vitro study. *Clin Oral Implants Res.* (2018) 29:835–42.
5. Pujari M, Garg P, Prithviraj D. Evaluation of accuracy of casts of multiple internal connection implant prosthesis obtained from different impression materials and techniques: an in vitro study. *J Oral Implantol.* (2014) 40:137–45.
6. Papaspyridakos P, Gallucci G, Chen C, Hanssen S, Naert I, Vandenberghe B. Digital versus conventional implant impressions for edentulous patients: accuracy outcomes. *Clin Oral Implants Res.* (2016) 27:465–72.
7. Jemt T, Hjalmarsson L. In vitro measurements of precision of fit of implant-supported frameworks. A comparison between "virtual" and "physical" assessments of fit using two different techniques of measurements. *Clin Implant Dent Relat Res.* (2012) 14:e175–82.
8. Lee S, Betensky R, Gianneschi G, Gallucci G. Accuracy of digital versus conventional implant impressions. *Clin Oral Implants Res.* (2015) 26:715–9.
9. Lee H, So J, Hochstedler J, Ercoli C. The accuracy of implant impressions: a systematic review. *J Prosthet Dent.* (2008) 100:285–91.
10. Tafti A, Hatami M, Razavi F, Ebadian B. Comparison of the accuracy of open-tray and snap-on impression techniques of implants with different angulations. *Dent Res J.* (2019) 16:413–20.
11. Prithviraj D, Pujari M, Garg P, Shruthi D. Accuracy of the implant impression obtained from different impression materials and techniques: review. *J ClinExp Dent.* (2011) 3:e106–11.
12. Linkevicius T, Svediene O, Vindasiute E, Puisys A, Linkeviciene L. The influence of implant placement depth and impression material on the stability of an open tray impression coping. *J Prosthet Dent.* (2012) 108:238–43.
13. Güth J, Keul C, Stimmelmayr M, Beuer F, Edelhoff D. Accuracy of digital models obtained by direct and indirect data capturing. *Clin Oral Investig.* (2013) 17:1201–8.
14. Marghalani A, Weber H, Finkelman M, Kudara Y, El Rafie K, Papaspyridakos P. Digital versus conventional implant impressions for partially edentulous arches: An evaluation of accuracy. *J Prosthet Dent.* (2018) 119:574–9.
15. Nam N, Shin S, Lim J, Lee B, Shim J, Kim J. Accuracy of implant position reproduction according to exposed length of the scan body during optical scanning: An in vitro study. *Appl Sci.* (2021) 11:1689.
16. Papaspyridakos P, Vazouras K, Chen Y, Kotina E, Natto Z, Kang K, et al. Digital vs. Conventional Implant Impressions: A Systematic Review and Meta-Analysis. *J Prosthodont.* (2020) 29:660–78.
17. Marques S, Ribeiro P, Falcão C, Lemos BF, Ríos-Carrasco B, Ríos-Santos JV, et al. Digital Impressions in Implant Dentistry: A Literature Review. *Int J Environ Res Public Health.* (2021) 18:1020.
18. Cruz R, Lemos C, de Luna Gomes J, Fernandes E, Oliveira H, Pellizzer E, et al. Clinical comparison between crestal and subcrestal dental implants: A systematic review and meta-analysis. *J Prosthet Dent.* (2022) 127:408–17.
19. Ender A, Mehl A. Accuracy of complete-arch dental impressions: a new method of measuring trueness and precision. *J Prosthet Dent.* (2013) 109:121–8.
20. Hitendra S, Bhagyashree D, Setu P, Shruti M, Rahul B, Chirag V. An In-Vitro Study for Evaluating Accuracy of Replication of Implant Position with Different Implant Impression Techniques. *JOPD* (2020) 15:18–27.
21. Rutkūnas V, Gečiauskaitë A, Jegelevičius D, Vaitiekūnas M. Accuracy of digital implant impressions with intraoral scanners. A systematic review. *Eur J Oral Implantol.* (2017) 10:101–20.
22. Papaspyridakos P, Hirayama H, Chen C, Ho C, Chronopoulos V, Weber H. Full-arch implant fixed prostheses: a comparative study on the effect of connection type and impression technique on accuracy of fit. *Clin Oral Implants Res.* (2016) 27:1099–105.
23. DeLong R, Pintado M, Ko C, Hodges J, Douglas W. Factors influencing optical 3D scanning of vinyl polysiloxane impression materials. *J Prosthodont.* (2001) 10:78–85.
24. Lee H, Ercoli C, Funkenbusch P, Feng C. Effect of subgingival depth of implant placement on the dimensional accuracy of the implant impression: an in vitro study. *J Prosthet Dent.* (2008) 99:107–13.
25. Lee S, Jamjoom F, Le T, Radics A, Gallucci GO. A clinical study comparing digital scanning and conventional impression making for implant-supported prostheses: A crossover clinical trial. *J Prosthet Dent.* (2022) 128:42–8.
26. Mizumoto R, Yilmaz B. Intraoral scan bodies in implant dentistry: A systematic review. *J Prosthet Dent.* (2018) 120:343–52.